A positive feedback loop between TAZ and miR-942-3p modulates proliferation, migration, epithelial-mesenchymal transition process and glycometabolism in human bladder cancer

Feifan Wang
Zhejiang University School of Medicine First Affiliated Hospital
Mengjing Fan
Zhejiang University School of Medicine Sir Run Run Shaw Hospital
Xuejian Zhou
Zhejiang University School of Medicine First Affiliated Hospital
Yanlan Yu
Zhejiang University School of Medicine Sir Run Run Shaw Hospital
Yueshu Cai
Zhejiang University School of Medicine First Affiliated Hospital
Hongshen Wu
Zhejiang University School of Medicine First Affiliated Hospital
Yan Zhang
Zhejiang University School of Medicine First Affiliated Hospital
Jiaxin Liu
Zhejiang University School of Medicine First Affiliated Hospital
Shihan Huang
Zhejiang University School of Medicine First Affiliated Hospital
Ning He
Zhejiang University School of Medicine First Affiliated Hospital
Zhenghui Hu
Zhejiang University School of Medicine First Affiliated Hospital
Guoqing Ding
Zhejiang University School of Medicine Sir Run Run Shaw Hospital
Xiaodong Jin (xiaodong-jin@zju.edu.cn)
Zhejiang University School of Medicine First Affiliated Hospital https://orcid.org/0000-0003-2734-3882

Research

Keywords: Bladder cancer, TAZ, miR-942-3p, Progression, EMT, Glycometabolism

Posted Date: October 7th, 2020

DOI: https://doi.org/10.21203/rs.3.rs-86063/v1

Version of Record: A version of this preprint was published on January 26th, 2021. See the published version at https://doi.org/10.1186/s13046-021-01846-5.

Abstract

Background: Transcriptional co-activator with PDZ-binding motif (TAZ) has been reported to involve in tumor progression, epithelial-mesenchymal transition (EMT) process and glycometabolism modulation. Herein, the underlying molecular mechanisms of TAZ-induced biological effects in bladder cancer were discovered;

Methods: qRT-PCR, western blot and immunohistochemistry were performed to determine the level of TAZ in bladder cancer cells and tissues; CCK-8 assay, Colony formation assay, wound healing assay and Transwell assay were performed to evaluate the functions of TAZ, miR-942-3p and GAS1. qRT-PCR and western blot were used to determine the expression levels of related genes. Chromatin immunoprecipitation and dual-luciferase reporter assay confirmed the interaction between TAZ and miR-942. In vivo tumorigenesis assay and colorimetric assay of glycolysis were also conducted;

Results: We determined the upregulation and vital roles of TAZ in bladder cancer. TAZ-induced upregulation of miR-942-3p amplified upstream signaling by inhibiting the expression of large tumor suppressor 2 (LATS2, a TAZ inhibitor). MiR-942-3p attenuated the suppression of cell proliferation, EMT process and glycolysis induced by TAZ knockdown. Further, miR-942-3p resulted in restrained expression of growth arrest-specific 1 (GAS1) to modulate biological functions;

Conclusion: Our study identified a novel positive feedback loop between TAZ and miR-942-3p that regulates biological functions in bladder cancer cells via GAS1 expression, and illustrated that TAZ and miR-942-3p might be potential therapeutic targets for bladder cancer treatment.

Background

Bladder cancer is the ninth most common malignant tumor worldwide and ranks 13th in mortality from cancer every year. There were approximately 430,000 new-set cases in 2012[1–4]. Bladder cancer can be classified into to non-muscle invasive and muscle-invasive bladder cancer according to the depth of tumor infiltration[5,6]. Although timely surgical intervention and chemotherapy can restrict the progression and development of tumor, the 5-year overall survival rate of muscle-invasive bladder cancer patients is 60% due to distant metastasis[7]. Therefore, it is meaningful to clarify the molecular mechanisms underlying bladder cancer progression for discovering the novel and precise therapeutic targets and improving prognosis in bladder cancer.

In the past decades, numerous studies have confirmed the critical roles of Hippo pathway in tissue homeostasis, cell proliferation, apoptosis and multiple biological processes. Surprisingly, impairment of the Hippo pathway leads to a remarkable impact on cancer development, progression and metabolic phenotype[8–13]. The core of the Hippo pathway is composed of a kinase cascade, transcription coactivators, and DNA-binding partners. The pathway is regulated by intrinsic cell machineries and various cellular signals[14]. The upstream serine/threonine kinases Mst1/2 (mammalian sterile twenty-like)

can phosphorylate and activate Lats1/2 (large tumor suppressor) via a complex with the adaptor protein Sav1. Then activated Lats1/2, together with Mob1, suppresses transcriptional coactivators TAZ (transcriptional coactivator with PDZ-binding motif) and its paralogue YAP (Yes-associated protein) through phosphorylation[15]. TAZ interact with the TEA domain DNA-binding family of transcription factors (TEAD) to recruit to their target promoters and regulate gene expression[16]. In mammals, the transcriptional activation of TEADs requires transcriptional coactivators, such as TAZ, YAP and p160 family of nuclear receptor coactivators[17].

Epithelial-mesenchymal transition (EMT) plays essential roles during normal mammalian development in which epithelial cells acquire mesenchymal features. However, EMT is associated with tumorigenesis and metastasis and is unintentional in cancer progression [18–20]. Therefore, the EMT-related signaling pathways have been studied as a novel focus for cancer therapy in past decades[21–24]. Interestingly, emerging studies have demonstrated the regulatory role of the components in Hippo signaling pathway in EMT process[25–29].

MicroRNAs regulate the level of protein-coding genes by binding to the specific sequence of mRNAs[30]. A growing number of researches have reported that microRNAs involve in multiple aspects of biologic cellular processes, including cancer development and progression, making them novel therapeutic targets for treatment[24,31,32]. Moreover, the dysregulation of miRNAs and their influences on tumorigenesis, development, and progression have been discovered in bladder cancer[33,34].

GAS1 (Growth arrest-specific 1) is a well-known cell growth suppressor[35] and involves in tumorigenesis and progression[36–38]. Aberrant expression of GAS1 reduce tumorigenicity in human brain tumor-initiating cells[39], while downregulation of GAS1 is a potential biomarker of clear cell renal cell carcinoma[40]. Interestingly, GAS1 has been reported to serve as a novel biomarker and inhibit proliferation, EMT process and glycolysis in colorectal cancer[41].

In the current study, we investigated the abundant expression of TAZ in both bladder cancer cell lines and tissues. Besides, TAZ knockdown suppressed the proliferation, migration, EMT process and glycolysis of bladder cancer cells. Mechanically, we identified a positive feedback loop between TAZ and miR-942-3p, which enhanced upstream signals and modulated biological and metabolic phenotypes via regulating GAS1 expression. Collectively, our results indicated that TAZ, miR-942-3p and GAS1 are novel therapeutic targets in clinical intervention of bladder cancer patients.

Materials And Methods

Ethical approval

All animal experiments were approved by the Ethics Committee of The First Affiliated Hospital, Zhejiang University School of Medicine and were carried according to the guidelines of the Guide for the Care and Use of Laboratory Animals published by the NIH.

Clinical tissue specimens

Clinical tissue specimens and paired normal bladder tissues were acquired from the surgical specimens. All patients engaging in the study obtained written informed consent. All specimens were characterized by pathologists histologically according to the World Health Organization Consensus Classification and TNM staging system for bladder neoplasms. The study was performed according to the Ethics Committee of First Affiliated Hospital of Zhejiang University School of Medicine. Detailed information of patients is listed in Supplemental File 1. Table S1 and S2.

Cell lines and culture

SV-HUC-1, HEK-293 cells and human bladder cancer cell lines 5637, J82, T24, EJ, TCCSUP, RT4 and UM-UC-3 were acquired from the American Type Culture Collection. HEK-293 were cultured in 10% fatal bovine serum containing Dulbecco's modified Eagle's medium, and the other cells mentioned above were cultured in RPMI-1640 medium.

RNA extraction and quantitative real-time PCR

Total RNA was extracted by TRIzol Reagent (Invitrogen, CA, USA). For mRNA detection, the PrimeScript RT reagent Kit (Takara Bio Inc., China) was used for mRNA reverse transcription. qRT-PCR was performed by utilizing TB Green Premix Ex Taq II (Takara Bio Inc., China) with a QUANT5 PCR system (Applied Biosystems, USA). The normalized control of mRNA expression analysis was GAPDH. The All-in-One miRNA qRT-PCR detection kit (GeneCopoeia, USA) was applied For miRNA detection, and human U6 was performed as an endogenous control. Data analysis of the relative expression levels used the $2^{-\Delta\Delta Ct}$ method. The primers used are listed: **TAZ**: Fwd, 5'-ACCCGCGAGTACAACCTTCTT-3', and Rev, 5'-TATCGTCATCCATGGCGAACT-3'; **E-cadherin**: Fwd, 5'-CATGAGTGTCCCCCGGTATC-3', and Rev, 5'-CAGTATCAG CCGCTTTCAGA-3'; **N-cadherin**: Fwd, 5'- TTTGATGGAGGTCTCCTAACACC-3', and Rev, 5'-ACGTTTAACACGTTGGAAATGTG-3'; **Vimentin**: Fwd, 5'-AGTCCACTGAGTACCGGAGAC-3', and Rev, 5'-CATTTCACG CATCTGGCGTTC-3'; **Fibronectin**: Fwd, 5'-GGATGCTCCTGCTGTCAC-3', and Rev, 5'-CTGTTTGATCTGGACCTGCAG-3'; **Snail**: Fwd, 5'- ACTGCAACAAGGAATACCTCAG -3', and Rev, 5'-GCACTGGTACTTCTTGACATCTG -3'; **PFKFB3**: Fwd, 5'- CGACCCCGACAAATGCGACAG -3', and Rev, 5'-GTACACGATGCGGCTCTGGATG -3'; **LDHB**: Fwd, 5'- GAACTTGCTCTTGTGGATGTTT -3', and Rev, 5'-CTGAAGAAATAAGCTCCCATGC -3'; **HK2**: Fwd, 5'- CGTGCCCGCCAGAAGACATTAG -3', and Rev, 5'-CTTGCTCAGACCTCGCTCCATTTC -3'; **GLUT1**: Fwd, 5'- TGTCTGGCATCAACGCTGTCTTC -3', and Rev, 5'-CCTGCTCGCTCCACCACAAAC -3'; **GLUT3**: Fwd, 5'- CAAGAGCCCATCTATGCCACCATC -3', and Rev, 5'-AGAGTCCTTCTTCCTGCCCTTTCC -3'; **GLUT4**: Fwd, 5'- CTGAAGGATGAGAAGCGGAAG -3', and Rev, 5'-TCGAAGATGCTGGTCGAATAAT -3'; **GAPDH**: Fwd, 5'-GATATTGTTGCCATCAATGAC-3', and Rev, 5'-TTGATTTTGGAGGGATCTCG -3'; **miR-942-3p**: CACATGGCCGAAACAGAGAAGT.

siRNA, plasmid and lentivirus

siRNAs, TAZ, TEAD2, miR-942 promoter and GAS1 plasmids were constructed and obtained from Transheep (Shanghai, China). MiR-942-3p mimic was synthesized by RiboBio (Guangzhou, China). siRNA was transfected with Lipofectamine™ RNAiMAX Transfection Reagent (Invitrogen, USA), while plasmids were transfected with Lipofectamine™ 3000 Transfection Reagent (Invitrogen, USA), according to the manufacturer's instructions. Lentivirus-Pre-miR-942, Lentivirus-miR-942-3p-sponge and Lentivirus-shTAZ were all purchased from Genechem (Shanghai, China). Cells were transduced with lentiviruses and were selected with puromycin for one week.

Chromatin immunoprecipitation (ChIP)

The SimpleChIP® Plus Enzymatic Chromatin IP Kit (Catalog# 9004, Cell Signaling Technology, USA) was utilized for ChIP assay according to the manufacturer's instructions. Briefly, cells (4×10^6) were fixed with formaldehyde and lysed, and chromatin is fragmented by digestion with Micrococcal Nuclease to obtain fragments of 1-5 nucleosomes. Chromatin immunoprecipitations were performed using 2 μg antibodies and Protein G Agarose Beads with incubation overnight at 4℃ with rotation. The eluents from the immunoprecipitants were used for reversal of cross-links. Then, we purified DNA and performed qRT-PCR with specific primers. The sequence of primers for miR-942 promoter was listed: **Primer-1**: Fwd, 5'-TTTGCTCCCTTGACTCCCAGC-3', and Rev, 5'-GGTCAAAGCACTGAGCTGTTCTT-3'; **Primer-2**: Fwd, 5'-ATTGCACTGAAGTGGGTTTTCTGT-3', and Rev, 5'- GACACAGTCTCTAGAGTCAAGCCT-3'; **Primer-3**: Fwd, 5'-CCTTCAGAGTGAGCTATTGGGC-3', and Rev, 5'-CCTTCCCTACTTGAAACAACCGT-3'; **Primer-4**: Fwd, 5'-CTTCAGAGTGAGCTATTGGGCTAAAAT-3', and Rev, 5'-CCTTCCCTACTTGAAACAACCGTATG-3'; **Primer-5**:Fwd, 5'-CCAGCCATATGAGGACAGAGGAAG-3', and Rev, 5'-CTTTCAAGAGCCTCTAAGGGCCC-3'.

Luciferase reporter assay

For verifying the transcriptional activity of TAZ-TEAD on miR-942 promoter, 293T cells were plated in 96-well plates (5000 cells) and were co-transfected with Firefly luciferase plasmid miR-942 promoter, TEAD2 and TAZ plasmid (Transheep, China). pRL-CMV Renilla luciferase were also co-transfected to normalize the luciferase activities. Plasmids were transfected by Lipofectamine™ 3000 Transfection Reagent (Invitrogen, USA). Dual-luciferase Reporter Assay Detection Kit (Promega, USA) was performed for cell luciferase activities detection.

For confirmation the relationship between miR-942-3p and GAS1 or LATS2, a luciferase reporter vector (pGL3-Firefly_Luciferase-Renilla_Luciferase) with full length of the 3'-UTR of GAS1 or LATS2 was constructed and the mutant vectors were also generated (GeneChem, China). 293T cells were seeded and co-transfected with a luciferase vector and miR-942-3p mimic or negative control. The Dual-luciferase Reporter Assay Detection Kit (Promega, USA) was used for the firefly and Renilla luciferase activities measure.

Migration and invasion assays

Migration and invasion chamber (Costar, NY, USA) was used in migration and invasion assays. Briefly, 3 × 10^4 cells in serum-free medium were seeded into the upper chambers. Specifically, for invasion assay, Matrigel (BD, MA, USA) pre-coated upper chambers were used. The bottom chambers were added with 10% fetal bovine serum containing medium. Migrated and invasive cells were fixed with fomalin and stained with crystal violet. The stained cells were observed and counted by microscopy (200×) in five randomly selected fields.

Wound healing assay

Bladder cancer cells were plated into Culture-Insert (ibidi, Germany) according to manufacturer's instructions. After 24 h, Culture-Inserts were removed and the cells were incubated in serum free medium. Photos were captured at 0 and 24 h after insert removed and the migration rate of the cells was measured by Image J software.

Apoptosis analysis

Cells with different condition were counted and stained with Annexin V-FITC and PI. The apoptotic rate of cells was detected by flow cytometry (Becton Dickinson, USA) after incubation for 30 min at room temperature.

Western blot analysis and antibodies

Total proteins were extracted by using RIPA buffer (C1053, APPLYGEN, Beijing, China), and protein concentration measurement was performed. Proteins were then separated by SDS-PAGE and transferred to PVDF membranes (Millipore, Billerica, MA). After blocked for 2 h in 5% milk, the membrane was rinsed with TBST for 3 times and was incubated with primary antibodies at 4°C overnight. The membrane was then incubated with secondary antibody (anti-mouse or anti-rabbit IgG，Cell Signaling Technology, USA) for 1 h at room temperature. A Bio-Rad detection system was used to detect the bands. The antibodies used in this study were as follows: anti-GAPDH (5174), anti-TAZ (70148), anti-E-cadherin (3195), anti-Snail (3879), anti-N-cadherin (13116), anti-Vimentin (5741) and anti-Fibronectin (26836) were all obtained from Cell Signaling Technology. Anti-LATS2 (ab110780), anti-GAS1 (ab236618), anti-PFKFB3 (ab181861), anti-HK2 (ab209847) and anti-GLUT1 (ab115730) were all obtained from Abcam.

Glycolysis process evaluation

The uptake of Glucose in different cells was determined by Glucose Uptake Colorimetric Assay Kit (Biovision, CA, USA). The production of lactate was detected by using Lactate Colorimetric Assay Kit (Solarbio, Beijing, China). All the procedures were carried out according to the manufactures' instructions.

Other in vitro experiments

CCK-8 assay, colony formation assay and HE staining were performed according to previously described methods[24].

In vivo studies

For establishment of xenograft tumorigenesis model, 5×10^6 of T24 cells with different treatments were injected subcutaneously into nude mice. The mice were sacrificed and the tumors were excised, weighed, and fixed with formalin for immunohistochemical examination 25 days later. Tumor sizes were measured daily and calculated by the following formula: Total tumor volume (mm^3) = $L\times W^2/2$ ("L" = length and "W" = width). All animal-related procedures were approved by the Animal Care and Use Committee of The First Affiliated Hospital of the School of Medicine of Zhejiang University.

Statistical analysis

All data were expressed as the mean ± standard deviation (SD) and were analyzed with SPSS. A paired t-test was used to analyze the difference expression in both cells and tissues. A two-tailed p-value < 0.05 was regarded as statistically significant in this study.

Results

TAZ expression is markedly elevated in bladder cancer cells lines and tissue

First, we investigated TAZ expression difference between human bladder cancer tissues and their matched adjacent normal tissues (cohort 1, n=20). As shown in Fig. 1a and 1b, TAZ was overexpressed in the bladder cancer tissues at both mRNA and protein levels. Meanwhile, the data in TCGA database represented the similar trend (Fig. 1c). We then detected TAZ level in SV-HUC-1 and bladder cancer cell lines. The results revealed that TAZ was markedly upregulated in bladder cancer cell lines compared with normal human uroepithelium cells (Fig. 1d and 1e). Furthermore, we performed immunohistochemical assay and found that TAZ was higher in bladder cancer tissue than that in adjacent normal tissue in cohort 2 (n=30, Fig. 1f).

TAZ knockdown suppresses proliferation, colony formation, migration, invasion and mesenchymal transformation of bladder cancer cells

To evaluated the potential roles of TAZ in bladder cancer cells, we used a short interfering RNA (siRNA) to deplete TAZ expression. The efficiency of siRNAs was evaluated by western blotting in T24 cells (Fig. 2a). CCK-8 assay and colony-formation assay demonstrated that TAZ knockdown suppressed cell proliferation and colony-forming ability (Fig. 2b and 2c). Wound healing assay indicated that TAZ was involved in bladder cancer cell migration (Fig. 2d). In addition, depletion of TAZ significantly decreased migrated cells in Transwell migration and Matrigel invasion assays in T24 and EJ cells (Fig. 2e). Previous researches have reported that cell migration and EMT process are closely associated with tumor migration, invasion, progression and metastasis[18-20,22]. Interestingly, we found that TAZ expression was positively correlated with that of mesenchymal markers (Vimentin, N-cadherin, Fibronectin and Snail) and negatively correlated with that of epithelial marker (E-cadherin) (Fig. 2f). The above results indicated the key role of TAZ in EMT process. As we predicted, TAZ inhibition led to downregulation of N-cadherin,

Vimentin, Fibronectin and Snail and upregulation of E-cadherin at protein level and mRNA level (Fig. 2g and 2h). Our current results demonstrated that TAZ served as a vital regulator in various biological functions of bladder cancer cell.

Inhibition of TAZ suppresses glycolysis via regulating PFKFB3, HK2 and GLUT1 expression in bladder cancer cells

Numerous researches have reported that Hippo pathway is involved in glucose metabolism[12,13]. Meanwhile, the specific metabolic phenotype is well accepted as a characteristic of tumor cells. Therefore, we evaluated the role of TAZ in glycometabolism of bladder cancer cells. Fig. 2i illustrated the process of aerobic glycolysis. As shown in Fig. 2j and 2k, inhibition of TAZ significantly decreased uptake of glucose and production of lactate, which indicated the suppression of glycolysis. In addition, we also detected the expression levels of several glycolysis-related genes to clarify the underlying regulatory mechanism of TAZ on glycolysis. The results demonstrated that TAZ knockdown could decrease the levels of PFKFB3, HK2 and GLUT1 at mRNA level and protein level (Fig. 2l and 2m). These results illustrated that TAZ might function as a key factor in aerobic glycolysis of bladder cancer.

MiR-942-3p is regulated by TAZ-TEAD

To clarify the greater details about regulatory mechanism of TAZ in bladder cancer, we verified miRNAs regulated by TAZ in T24 bladder cancer cells by RNA sequencing (Fig. 3a and Supplemental File 2). Among the downregulated miRNAs induced by TAZ knockdown, we found that miR-942-3p has been reported to be a key factor in cell proliferation and invasion[42,43] and selected miR-942-3p as our research subject. qRT-PCR was used to confirm the remarkable downregulated miR-942-3p in TAZ-knockdown bladder cancer cells (Fig. 3b). Furthermore, TAZ overexpression could enhance the miR-942-3p expression (Fig. 3c). Besides, the expression levels of TAZ and miR-942-3p were positively correlated both in cohort 1 and TCGA database (Fig. 3d and 3e). We also found the alternations of miR-942-3p in LATS1 and LATS2 or TEAD2 knockdown cells, which indicated that Hippo signaling pathway play a key role in TAZ/miR-942-3p regulatory mechanism (Fig. 3f and 3g). TAZ interacts with the TEAD to recruit to their target promoters and regulate gene expression[16,17,44]. Therefore, we predicted the binding site of TEADs in the promoter region of miR-942 in JASPAR (Fig. 3h). We then performed chromatin immunoprecipitation (ChIP) to investigate the interaction between TAZ and miR-942 promoter. qRT-PCR detection for miR-942 promoter was performed and analyzed by employing different primers (indicated in Fig. 3h). As shown in Fig. 3i, TAZ could enrich the DNA segments containing the predicted TEADs binding site, which could be amplified by using primer 3 and 4. Luciferase reporter assay further confirmed that the ability of TAZ-TEAD2 to activate the promoter of miR-942 depending on the presence of the TEAD-binding sequence (Fig. 3j). In summary, these results verified that miR-942 was a direct target of TAZ-TEAD.

MiR-942-3p acts as a tumor promotor in bladder cancer

We first detected the expression level of miR-942-3p in bladder cancer cells and tissues. The results confirmed the upregulation of miR-942-3p in bladder cancer tissues (cohort 1) and cell lines (Fig. 4a-c),

which indicated that miR-942-3p was associated with tumorigenesis and progression in bladder cancer. To verify this hypothesis, we transfected T24 and EJ cells with Pre-miR-942 or miR-942-3p sponge. CCK-8 assay and colony formation assay revealed that miR-942-3p overexpression enhanced cell viability and proliferation, while miR-942-3p inhibition led to the opposite results (Fig. 4d and 4e). Besides, wound healing, Transwell migration and invasion assays were performed to evaluate the migratory and invasive abilities. The results showed that miR-942-3p acted as a promoter in bladder cancer cell migration and invasion (Fig. 4f and 4g). We also detected EMT markers by western blotting and qRT-PCR in miR-942-3p overexpression or knockdown cells to investigate whether EMT process was regulated by miR-942-3p. As shown in Fig. 4h and 4i, miR-942-3p enhanced the expression of E-cadherin and suppressed the expression of N-cadherin, Vimentin, Fibronectin and Snail at protein level and mRNA level. Conversely, miR-942-3p inhibition exhibited opposite effects in bladder cancer cells. Our data demonstrated that miR-942-3p was a TAZ-induced and abundantly expressed miRNA in bladder cancer, which played a significant role in cell migration, invasion and EMT process.

GAS1 and LATS2 act as direct targets of miR-942-3p in bladder cancer

We then identified the molecular mechanism of miR-942-3p in bladder cancer by predicting the target genes of miR-942-3p in several databases (TargetScan, miRWalk, miRDB and miRTarBase). Firstly, four lists of genes overlapped, and four genes were targeted by miR-942-3p in all the databases (Fig. 5a). GAS1 is a well-known cell growth suppressor and involves in tumorigenesis and progression[39-41,45]. Interestingly, apart from the above 4 genes, we found that LATS2, as a significant component of Hippo signaling pathway, was targeted by miR-942-3p in TargetScan. Therefore, GAS1 and LATS2 were selected for further verification. The potential binding sites of miR-942-3p within the 3'-untranslated regions (3'-UTRs) of GAS1 and LATS2 were showed in Fig. 5b. To validate whether miR-942-3p binds to these 3'-UTRs, we constructed luciferase reporter plasmids containing the full length 3'-UTR of GAS1 or LATS2 and their mutant types and co-transfected them with miR-942-3p mimics. MiR-942-3p mimics induced a remarkable reduction in luciferase activity of the wild type GAS1 and LATS2 3'-UTRs. Besides, the mutated forms of the above 3'-UTRs eliminated the reduction in luciferase activity induced by miR-942-3p mimics in wild type 3'-UTRs (Fig. 5c). In addition, GAS1 and LATS2 were negatively correlated with miR-942-3p in TCGA database and bladder cancer cell lines at mRNA level and protein level, respectively (Fig. 5d and 5e). These findings demonstrated that miR-942-3p specifically targets GAS1 and LATS2.

A TAZ/miR-942-3p positive feedback loop regulates the oncogenic effects of TAZ

Since LATS2 inhibits the activity of TAZ in Hippo signaling pathway, we considered that TAZ and miR-942-3p formed a positive feedback loop in bladder cancer. To verify this regulatory mechanism, we first investigated the biological functions in TAZ-knockdown cells with or without overexpressing miR-942-3p. Notably, upregulation of miR-942-3p partly attenuated the suppression of cell viability and proliferation induced by TAZ depletion (Fig. 6a and 6b). Transwell migration, Matrigel invasion assays along and wound healing assay indicated the rescue of migration and invasion abilities induced by miR-942-3p in TAZ-depleted cells (Fig. 6c and 6d). Additionally, the alternations in E-cadherin, Vimentin, N-cadherin,

Fibronectin and Snail at protein level and mRNA level demonstrated that EMT process were reversed by miR-942-3p in TAZ knockdown cells (Fig. 6e and 6f). Moreover, the miR-942-3p-mediated expression levels of LATS2, GAS1 and TAZ were also indicated in Fig. 6e. We then verified whether miR-942-3p could reverse the metabolic phenotype induced by TAZ knockdown. The results of glucose uptake and lactate production assays showed that glycolysis was enhanced by miR-942-3p in TAZ-deficient cells (Fig. 6g and 6h). PFKFB3, HK2 and GLUT1 were also upregulated by miR-942-3p at mRNA level and protein level (Fig. 6i and 6j). In summary, our results proved that a positive feedback loop between TAZ and miR-942-3p was involved in biological functions, EMT process and glycometabolism of bladder cancer cells.

GAS1 suppresses the aggressive characteristics and glycolysis of bladder cancer cells

We assessed the effects of GAS1 in bladder cancer cells by constructing stable GAS1-overexpressing cells via transducing lentivirus. CCK-8 assay and colony formation assay showed that GAS1 inhibited cell viability and proliferation of bladder cancer cells (Fig. 7a and 7b). Moreover, overexpressing GAS1 significantly reduced the relative percentage of wound closure (Fig. 7c). Transwell migration and invasion assays further reflected the attenuation of migration and invasion induced by GAS1 overexpression in T24 and EJ (Fig. 7d). To demonstrate whether GAS1 suppressed migration and invasion by regulating EMT process, we assessed the level of EMT markers expression at protein level and mRNA level. The results indicated that overexpression of GAS1 enhanced E-cadherin expression and decreased the levels of Vimentin, N-cadherin, Fibronectin and Snail (Fig. 7e and 7f). Furthermore, the detections of glucose uptake and lactate production showed that GAS1 inhibited cellular glycolysis (Fig. 7g and 7h). qRT-PCR and western blotting indicated the downregulations of PFKFB3, HK2 and GLUT1 at mRNA level and protein level (Fig. 7i and 7j), which were consistent with previous results induced by TAZ inhibition. In addition, both TCGA database (Fig. 7k) and immunohistochemical detection for GAS1 in cohort 2 demonstrated the dysregulation of GAS1 in bladder cancer (Fig. 7l).

MiR-942-3p and TAZ promotes the growth of xenograft tumors in vivo

To verify the relationship between TAZ and miR-942-3p in vivo, we injected the cells with different condition (negative control, TAZ knockdown or sh-TAZ with miR-942 overexpression) into nude mice subcutaneously. Tumor volumes were measured every five days after injection. As shown in Fig. 8a-c, depletion of TAZ remarkably suppressed tumor growth rate and weight compared with the control group. Besides, overexpression of miR-942-3p abrogated the inhibited effects induced by TAZ knockdown. MiR-942-3p levels of tumor tissue in three groups were confirmed by performing qRT-PCR (Fig. 8d). We next assessed the expression level of TAZ, LATS2 and GAS1 in vivo. Immunochemical assay and western blotting indicated that TAZ knockdown upregulated the levels of LATS2 and GAS1 in tumor tissue, and miR-942-3p could reverse the trend (Fig. 8e and 8f). These results confirmed that miR-942-3p is vital for tumor growth mediated by TAZ in vivo. To illustrate our results more clearly, we created a schematic of TAZ/miR-942-3p regulatory model in Fig. 8g.

Discussion

TAZ is a key executor of the Hippo signaling pathway to regulate cellular proliferation, differentiation and tissue homeostasis[46,47]. In the past decades, a great deal of evidence indicated that dysregulation of TAZ contributed to cancer initiation and progression[48,49]. The present study confirmed that TAZ was overexpressed in bladder cancer cell lines and tissue and was related to cell proliferation, migration and invasion.

EMT are trans-differentiation programs in which epithelial cells acquire mesenchymal features. Interestingly, recent studies indicated that different state of EMT regulated tumor migration, invasion, metastasis and resistance to clinical therapy. Moreover, EMT might lead to the emergence of cancer stem cells and triggered tumor initiation[18,20,25,27,50]. Hippo signaling pathway has been reported to regulate EMT process and mesenchymal characteristics[51-54]. In the light of this, we examined EMT markers such as E-cadherin, Vimentin, N-cadherin, Fibronectin and Snail and found that TAZ knockdown reversed EMT process. It is well known that numerous pathways and factors are involved in modulation of EMT and therefore further study is needed to validate the exact regulatory mechanism in TAZ-induced EMT process.

TAZ and Hippo pathway are also participated in metabolism modulation, such as to regulate glycolysis, lipogenesis, and glutaminolysis[10-13]. Interestingly, a growing body of evidence has verified that glycometabolism might modulate cell growth, migration and progression in bladder cancer[55-57]. Actually, while normal cells acquire energy for physiological processes from the oxidation of pyruvate, cancer cells rely on aerobic glycolysis to generate energy and compound for their aberrant growth and metastasis. This metabolic characteristic of cancer cells is termed as the Warburg effect. The Warburg effect not only ensures the supply of energy and nutrients, but also provides an acidic microenvironment that enhances migration and invasion[58]. Therefore, it is meaningful to clarify the underlying mechanism of glycolysis in bladder cancer for clinical intervention and treatment. Our current results suggested that TAZ was vital for glycolysis of bladder cancer cells by regulating the expression of PFKFB3, HK2 and GLUT1, which serves as key components in glycolysis. However, the deeper relationship between glycolysis and other biological effects mediated by TAZ is worth exploring and verifying in the future study.

The TEAD protein family consists of four paralogous factors that function as nuclear DNA-binding proteins to modulate transcriptional activity of downstream genes in response to Hippo signaling pathway. Of note, the modulated role of TEAD depends on binding with TAZ or YAP in nucleus whose nuclear importation is mediated by LATS1/2[16,17,44]. MiRNAs participate in numerous biological processes, including tumor initiation, progression and metastasis[24,32-34,59]. Nevertheless, the underlying mechanism of dysregulated miRNAs in bladder cancer remains unclear. Therefore, we speculated that TAZ might exert its biological functions via enhancing the expression of miRNAs, and following miRNA sequencing, qRT-PCR, ChIP and luciferase reporter assays illustrated that miR-942-3p was regulated by TAZ-TEADs in bladder cancer cells. MiR-942 has been confirmed to play a key role in cancer[42,43]. Our results found that miR-942-3p was abundantly expressed in bladder cancer cell lines and tissue and served as a tumor promoter. Moreover, GAS1 and LATS2 were verified as downstream targets of miR-942-

3p directly. LATS2 could suppress the transcriptional activation of Hippo pathway-related gene by phosphorylating TAZ[9,14,44]. Interestingly, GAS1 acted as a key regulator in cell migration, EMT and glycometabolism in colorectal cancer cells[41]. Based on previous literatures and these results, our further experiments identified a positive feedback loop between TAZ and miR-942-3p and the biological effects of GAS1.

Conclusion

In summary, the present study verified a novel positive feedback loop between TAZ and miR-942-3p that regulates GAS1 expression and modulates biological behaviors, EMT process and glycometabolism in bladder cancer. TAZ, miR-942-3p and GAS1 might be potential therapeutic targets in clinical interventions of bladder cancer.

Abbreviations

TAZ: Transcriptional co-activator with PDZ-binding motif; GAS1: Growth arrest-specific 1; EMT: Epithelial-mesenchymal transition; miRNA: Micro RNA; sh-RNA: Small hairpin RNA; siRNA: Small interfering RNA; 3'-UTR: 3'- untranslated region; qRT-PCR: Quantitative real-time PCR; FBS: Fetal bovine serum; H&E: Hematoxylin and eosin; CCK-8: Cell Counting Kit-8; IHC: Immunohistochemistry.

Declarations

Ethics approval and consent to participate

The present study was approved by Ethics Committee of The First Affiliated Hospital l, School of Medicine, Zhejiang University and the Animal Research Ethics Committee of Zhejiang University.

Consent for publication

All authors have agreed with publishing this manuscript.

Availability of data and materials

The datasets used and/or analyzed in this article were included within the article and the additional files. Please contact the corresponding author for data requests.

Competing interests

The authors declare that they have no competing interests.

Funding

This work was supported by National Natural Science Foundation of China, Grant/Award Number: 81370799, Xiaodong Jin; Grant/Award Number: 81900595, Ning He. The Natural Science Foundation of

Zhejiang Province also supported this work, grant number: LY18H160013.

Authors' contributions

XDJ, GQD and FFW conceived of the study and carried out its design. FFW, MJF, YSC, XJZ and NH performed the experiments. FFW, MJF, HSW, YZ, JXL and SHH conducted the statistical analyses. FFW and YLY wrote the paper and XDJ and ZHH revised the paper. All authors read and approved the manuscript.

Acknowledgements

We thank Dr. Mengjing Fan from the Department of Pathology, Sir Run Run Shaw Hospital, Zhejiang University School of Medicine for establishing animal models. We also thank Dr. Yanlan Yu and Dr. Guoqing Ding from Department of Urology, Sir Run Run Shaw Hospital, Zhejiang University School of Medicine for providing us with condition of animal experiments.

References

1 Burge, F. & Kockelbergh, R. Closing the Gender Gap: Can We Improve Bladder Cancer Survival in Women? - A Systematic Review of Diagnosis, Treatment and Outcomes. *Urol Int* **97**, 373-379, doi:10.1159/000449256 (2016).

2 Dobruch, J. *et al.* Gender and Bladder Cancer: A Collaborative Review of Etiology, Biology, and Outcomes. *Eur Urol* **69**, 300-310, doi:10.1016/j.eururo.2015.08.037 (2016).

3 Thorstenson, A. *et al.* Gender-related differences in urothelial carcinoma of the bladder: a population-based study from the Swedish National Registry of Urinary Bladder Cancer. *Scand J Urol* **50**, 292-297, doi:10.3109/21681805.2016.1158207 (2016).

4 Antoni, S. *et al.* Bladder Cancer Incidence and Mortality: A Global Overview and Recent Trends. *Eur Urol* **71**, 96-108, doi:10.1016/j.eururo.2016.06.010 (2017).

5 Kamat, A. M. *et al.* Bladder cancer. *Lancet* **388**, 2796-2810, doi:10.1016/S0140-6736(16)30512-8 (2016).

6 Sanli, O. *et al.* Bladder cancer. *Nat Rev Dis Primers* **3**, 17022, doi:10.1038/nrdp.2017.22 (2017).

7 Soloway, M. S. Bladder cancer: Lack of progress in bladder cancer–what are the obstacles? *Nat Rev Urol* **10**, 5-6, doi:10.1038/nrurol.2012.219 (2013).

8 Yu, F. X., Zhao, B. & Guan, K. L. Hippo Pathway in Organ Size Control, Tissue Homeostasis, and Cancer. *Cell* **163**, 811-828, doi:10.1016/j.cell.2015.10.044 (2015).

9 Maugeri-Sacca, M. & De Maria, R. The Hippo pathway in normal development and cancer. *Pharmacol Ther* **186**, 60-72, doi:10.1016/j.pharmthera.2017.12.011 (2018).

10 Zheng, X. *et al.* LncRNA wires up Hippo and Hedgehog signaling to reprogramme glucose metabolism. *Embo j* **36**, 3325-3335, doi:10.15252/embj.201797609 (2017).

11 Cox, A. G. *et al.* Yap regulates glucose utilization and sustains nucleotide synthesis to enable organ growth. *Embo j* **37**, doi:10.15252/embj.2018100294 (2018).

12 Koo, J. H. & Guan, K. L. Interplay between YAP/TAZ and Metabolism. *Cell Metab* **28**, 196-206, doi:10.1016/j.cmet.2018.07.010 (2018).

13 Zhang, X. *et al.* The role of YAP/TAZ activity in cancer metabolic reprogramming. *Mol Cancer* **17**, 134, doi:10.1186/s12943-018-0882-1 (2018).

14 Meng, Z., Moroishi, T. & Guan, K. L. Mechanisms of Hippo pathway regulation. *Genes Dev* **30**, 1-17, doi:10.1101/gad.274027.115 (2016).

15 Zhao, B., Li, L., Lei, Q. & Guan, K. L. The Hippo-YAP pathway in organ size control and tumorigenesis: an updated version. *Genes Dev* **24**, 862-874, doi:10.1101/gad.1909210 (2010).

16 Lin, K. C. *et al.* Regulation of Hippo pathway transcription factor TEAD by p38 MAPK-induced cytoplasmic translocation. *Nat Cell Biol* **19**, 996-1002, doi:10.1038/ncb3581 (2017).

17 Lin, K. C., Park, H. W. & Guan, K. L. Regulation of the Hippo Pathway Transcription Factor TEAD. *Trends Biochem Sci* **42**, 862-872, doi:10.1016/j.tibs.2017.09.003 (2017).

18 De Craene, B. & Berx, G. Regulatory networks defining EMT during cancer initiation and progression. *Nat Rev Cancer* **13**, 97-110, doi:10.1038/nrc3447 (2013).

19 Diepenbruck, M. & Christofori, G. Epithelial-mesenchymal transition (EMT) and metastasis: yes, no, maybe? *Curr Opin Cell Biol* **43**, 7-13, doi:10.1016/j.ceb.2016.06.002 (2016).

20 Pastushenko, I. & Blanpain, C. EMT Transition States during Tumor Progression and Metastasis. *Trends Cell Biol* **29**, 212-226, doi:10.1016/j.tcb.2018.12.001 (2019).

21 Lemasters, J. J. The mitochondrial permeability transition: from biochemical curiosity to pathophysiological mechanism. *Gastroenterology* **115**, 783-786 (1998).

22 Singh, M., Yelle, N., Venugopal, C. & Singh, S. K. EMT: Mechanisms and therapeutic implications. *Pharmacol Ther* **182**, 80-94, doi:10.1016/j.pharmthera.2017.08.009 (2018).

23 Xu, Z. *et al.* Sodium Butyrate Inhibits Colorectal Cancer Cell Migration by Downregulating Bmi-1 Through Enhanced miR-200c Expression. *Mol Nutr Food Res* **62**, e1700844, doi:10.1002/mnfr.201700844 (2018).

24 Wang, F. *et al.* Sodium butyrate inhibits migration and induces AMPK-mTOR pathway-dependent autophagy and ROS-mediated apoptosis via the miR-139-5p/Bmi-1 axis in human bladder cancer cells. *FASEB J*, doi:10.1096/fj.201902626R (2020).

25 Han, L. L., Yin, X. R. & Zhang, S. Q. miR-103 promotes the metastasis and EMT of hepatocellular carcinoma by directly inhibiting LATS2. *Int J Oncol* **53**, 2433-2444, doi:10.3892/ijo.2018.4580 (2018).

26 Hu, Y. *et al.* miR-665 promotes hepatocellular carcinoma cell migration, invasion, and proliferation by decreasing Hippo signaling through targeting PTPRB. *Cell Death Dis* **9**, 954, doi:10.1038/s41419-018-0978-y (2018).

27 Yao, P. *et al.* ANKHD1 silencing suppresses the proliferation, migration and invasion of CRC cells by inhibiting YAP1-induced activation of EMT. *Am J Cancer Res* **8**, 2311-2324 (2018).

28 Braitsch, C. M. *et al.* LATS1/2 suppress NFkappaB and aberrant EMT initiation to permit pancreatic progenitor differentiation. *PLoS Biol* **17**, e3000382, doi:10.1371/journal.pbio.3000382 (2019).

29 Karvonen, H., Barker, H., Kaleva, L., Niininen, W. & Ungureanu, D. Molecular Mechanisms Associated with ROR1-Mediated Drug Resistance: Crosstalk with Hippo-YAP/TAZ and BMI-1 Pathways. *Cells* **8**, doi:10.3390/cells8080812 (2019).

30 Carthew, R. W. & Sontheimer, E. J. Origins and Mechanisms of miRNAs and siRNAs. *Cell* **136**, 642-655, doi:10.1016/j.cell.2009.01.035 (2009).

31 Kloosterman, W. P. & Plasterk, R. H. The diverse functions of microRNAs in animal development and disease. *Dev Cell* **11**, 441-450, doi:10.1016/j.devcel.2006.09.009 (2006).

32 Trang, P., Weidhaas, J. B. & Slack, F. J. MicroRNAs as potential cancer therapeutics. *Oncogene* **27 Suppl 2**, S52-57, doi:10.1038/onc.2009.353 (2008).

33 Chen, Z. *et al.* miR-190b promotes tumor growth and metastasis via suppressing NLRC3 in bladder carcinoma. *FASEB J*, doi:10.1096/fj.201901764R (2020).

34 Jin, H. *et al.* Oncogenic role of MIR516A in human bladder cancer was mediated by its attenuating PHLPP2 expression and BECN1-dependent autophagy. *Autophagy*, 1-15, doi:10.1080/15548627.2020.1733262 (2020).

35 Del Sal, G., Ruaro, M. E., Philipson, L. & Schneider, C. The growth arrest-specific gene, gas1, is involved in growth suppression. *Cell* **70**, 595-607, doi:10.1016/0092-8674(92)90429-g (1992).

36 Ma, Y., Qin, H. & Cui, Y. MiR-34a targets GAS1 to promote cell proliferation and inhibit apoptosis in papillary thyroid carcinoma via PI3K/Akt/Bad pathway. *Biochem Biophys Res Commun* **441**, 958-963, doi:10.1016/j.bbrc.2013.11.010 (2013).

37 Mo, H. *et al.* WT1 is involved in the Akt-JNK pathway dependent autophagy through directly regulating Gas1 expression in human osteosarcoma cells. *Biochem Biophys Res Commun* **478**, 74-80, doi:10.1016/j.bbrc.2016.07.090 (2016).

38 Gao, L., Wang, S., Meng, J. & Sun, Y. LncRNA LUADT1 Promotes Oral Squamous Cell Carcinoma Cell Proliferation by Regulating miR-34a/GAS1 Axis. *Cancer Manag Res* **12**, 3401-3407, doi:10.2147/cmar.S238830 (2020).

39 Sarkar, S. *et al.* Microglia induces Gas1 expression in human brain tumor-initiating cells to reduce tumorigenecity. *Sci Rep* **8**, 15286, doi:10.1038/s41598-018-33306-0 (2018).

40 Conceicao, A. L. *et al.* Downregulation of OCLN and GAS1 in clear cell renal cell carcinoma. *Oncol Rep* **37**, 1487-1496, doi:10.3892/or.2017.5414 (2017).

41 Li, Q. *et al.* Gas1 Inhibits Metastatic and Metabolic Phenotypes in Colorectal Carcinoma. *Mol Cancer Res* **14**, 830-840, doi:10.1158/1541-7786.MCR-16-0032 (2016).

42 Yang, D. *et al.* MiR-942 mediates hepatitis C virus-induced apoptosis via regulation of ISG12a. *PLoS One* **9**, e94501, doi:10.1371/journal.pone.0094501 (2014).

43 Xu, C. Y., Dong, J. F., Chen, Z. Q., Ding, G. S. & Fu, Z. R. MiR-942-3p Promotes the Proliferation and Invasion of Hepatocellular Carcinoma Cells by Targeting MBL2. *Cancer Control* **26**, 1073274819846593, doi:10.1177/1073274819846593 (2019).

44 Holden, J. K. & Cunningham, C. N. Targeting the Hippo Pathway and Cancer through the TEAD Family of Transcription Factors. *Cancers (Basel)* **10**, doi:10.3390/cancers10030081 (2018).

45 Sanchez-Hernandez, L., Hernandez-Soto, J., Vergara, P., Gonzalez, R. O. & Segovia, J. Additive effects of the combined expression of soluble forms of GAS1 and PTEN inhibiting glioblastoma growth. *Gene Ther* **25**, 439-449, doi:10.1038/s41434-018-0020-0 (2018).

46 Hansen, C. G., Moroishi, T. & Guan, K. L. YAP and TAZ: a nexus for Hippo signaling and beyond. *Trends Cell Biol* **25**, 499-513, doi:10.1016/j.tcb.2015.05.002 (2015).

47 Moya, I. M. & Halder, G. Hippo-YAP/TAZ signalling in organ regeneration and regenerative medicine. *Nat Rev Mol Cell Biol* **20**, 211-226, doi:10.1038/s41580-018-0086-y (2019).

48 Moroishi, T., Hansen, C. G. & Guan, K. L. The emerging roles of YAP and TAZ in cancer. *Nat Rev Cancer* **15**, 73-79, doi:10.1038/nrc3876 (2015).

49 Zanconato, F., Cordenonsi, M. & Piccolo, S. YAP/TAZ at the Roots of Cancer. *Cancer Cell* **29**, 783-803, doi:10.1016/j.ccell.2016.05.005 (2016).

50 Singh, A. & Settleman, J. EMT, cancer stem cells and drug resistance: an emerging axis of evil in the war on cancer. *Oncogene* **29**, 4741-4751, doi:10.1038/onc.2010.215 (2010).

51 Lei, Q. Y. *et al.* TAZ promotes cell proliferation and epithelial-mesenchymal transition and is inhibited by the hippo pathway. *Mol Cell Biol* **28**, 2426-2436, doi:10.1128/mcb.01874-07 (2008).

52 Cordenonsi, M. *et al.* The Hippo transducer TAZ confers cancer stem cell-related traits on breast cancer cells. *Cell* **147**, 759-772, doi:10.1016/j.cell.2011.09.048 (2011).

53 Li, Z. *et al.* The Hippo transducer TAZ promotes epithelial to mesenchymal transition and cancer stem cell maintenance in oral cancer. *Mol Oncol* **9**, 1091-1105, doi:10.1016/j.molonc.2015.01.007 (2015).

54 Tang, Y. & Weiss, S. J. Snail/Slug-YAP/TAZ complexes cooperatively regulate mesenchymal stem cell function and bone formation. *Cell Cycle* **16**, 399-405, doi:10.1080/15384101.2017.1280643 (2017).

55 Lea, M. A., Kim, H. & des, B. C. Effects of Biguanides on Growth and Glycolysis of Bladder and Colon Cancer Cells. *Anticancer Res* **38**, 5003-5011, doi:10.21873/anticanres.12819 (2018).

56 Xian, S., Shang, D., Kong, G. & Tian, Y. FOXJ1 promotes bladder cancer cell growth and regulates Warburg effect. *Biochem Biophys Res Commun* **495**, 988-994, doi:10.1016/j.bbrc.2017.11.063 (2018).

57 Chen, J., Cao, L., Li, Z. & Li, Y. SIRT1 promotes GLUT1 expression and bladder cancer progression via regulation of glucose uptake. *Hum Cell* **32**, 193-201, doi:10.1007/s13577-019-00237-5 (2019).

58 Liberti, M. V. & Locasale, J. W. The Warburg Effect: How Does it Benefit Cancer Cells? *Trends Biochem Sci* **41**, 211-218, doi:10.1016/j.tibs.2015.12.001 (2016).

59 Yoshino, H. *et al.* Aberrant expression of microRNAs in bladder cancer. *Nat Rev Urol* **10**, 396-404, doi:10.1038/nrurol.2013.113 (2013).

Figures

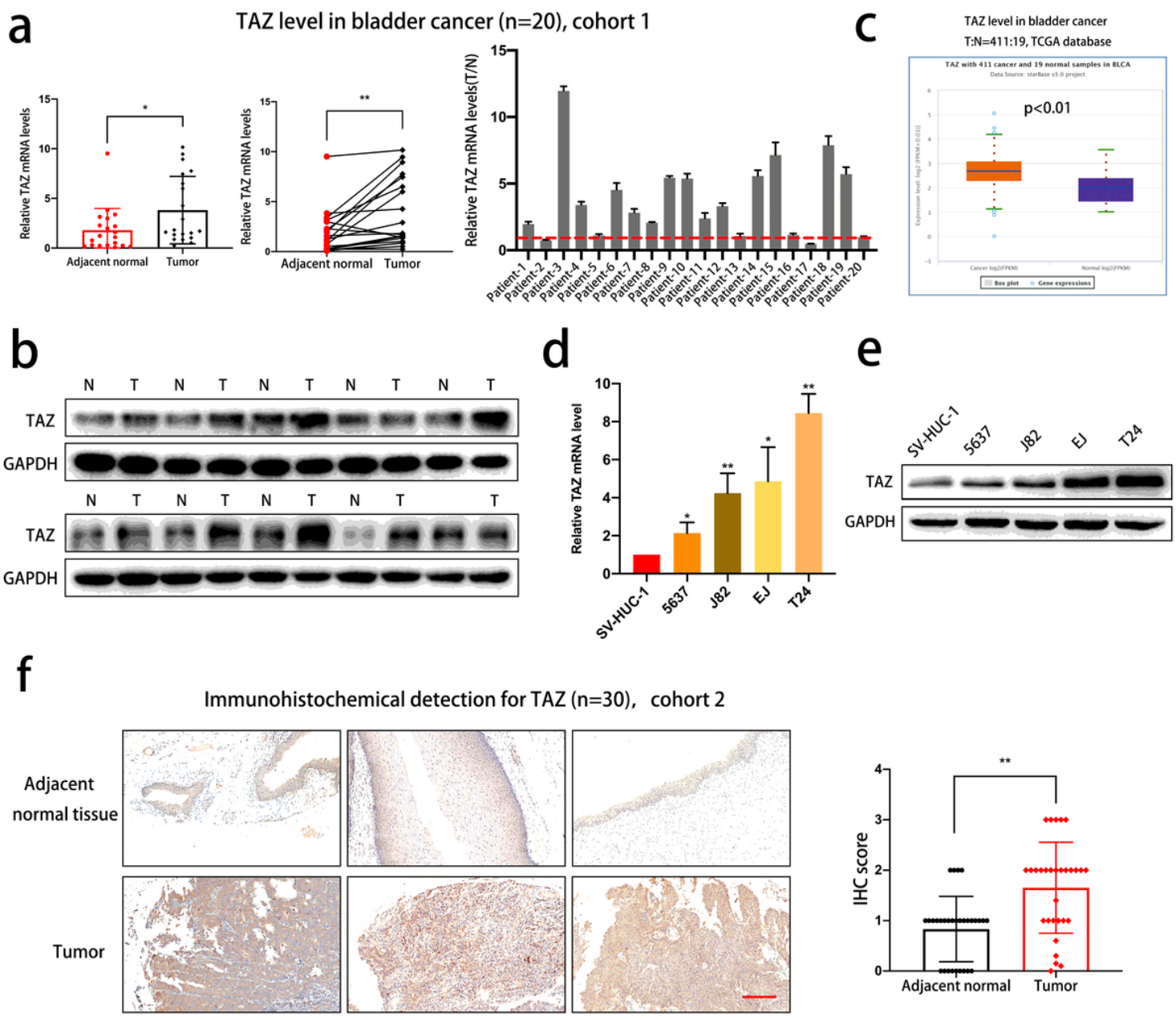

Figure 1

TAZ is overexpressed in bladder cancer cell lines and tissues a-b Detection of TAZ expression in human bladder cancer tissues and adjacent normal tissues at mRNA level and protein level (cohort 1, n=20). c. TAZ expression level of bladder cancer tissue and normal tissue in TCGA database. d-e TAZ expression levels were determined in SV-HUC-1 and different bladder cancer cell lines at mRNA level and protein level, respectively. f. The expression levels of TAZ in bladder cancer tissue were determined by IHC in cohort 2 (n=30). TAZ was significantly upregulated in bladder cancer tissue. Scale bar: 200 μm. *P < 0.05, **P < 0.01 vs. control group.

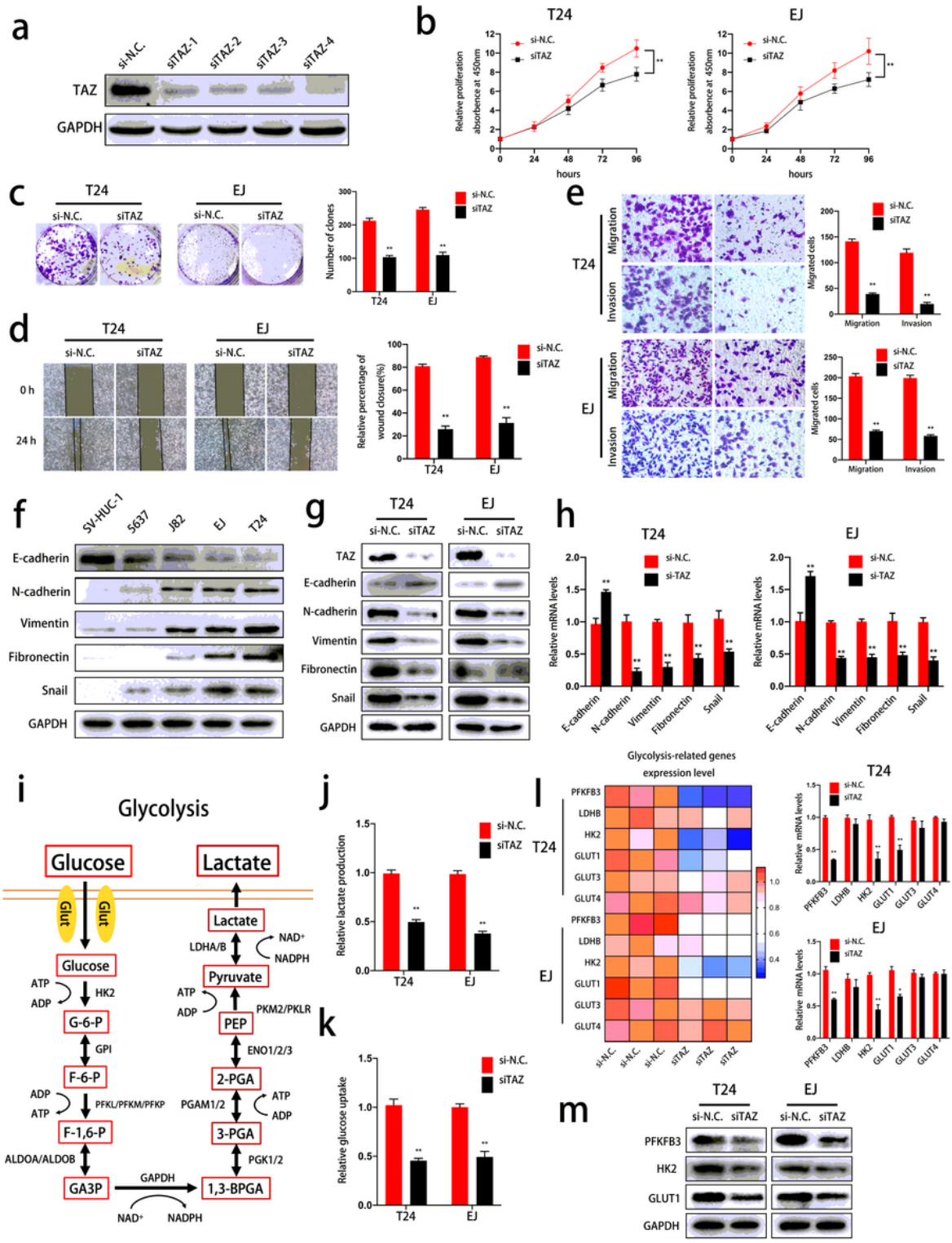

Figure 2

TAZ knockdown suppresses the proliferation, migration, invasion, EMT process and glycolysis of bladder cancer cells a. The knockdown efficiency of siRNAs for TAZ were determined by verified by western blotting in T24 cells. b. CCK-8 assay was performed to determine the effect of TAZ on cell viability. c. Depletion of TAZ inhibited the colony-forming ability of T24 and EJ cells. d. Wound healing assay was used to evaluate the cell migration ability in control or TAZ knockdown T24 and EJ cells. e. Cell migration

and invasion abilities of TAZ-deficient cells were evaluated by Transwell migration and invasion assays respectively. f. EMT markers were detected in SV-HUC-1 and bladder cancer cell lines by western blotting. g-h The key role of TAZ in EMT process was confirmed by western blotting and qRT-PCR. i. A schematic illustration of glycolysis was showed. j-k the uptake of glucose and the production of lactate in TAZ-deficient or normal bladder cancer cells were determined. l. qRT-PCR was performed to assess the expression levels of glycolysis-related genes (PFKFB3, LDHB, HK2, GLUT1, GLUT3 and GLUT4). m. The alternations of PFKFB3, HK2 and GLUT1 at protein level were confirmed by western blotting. *P < 0.05, **P < 0.01 vs. control group.

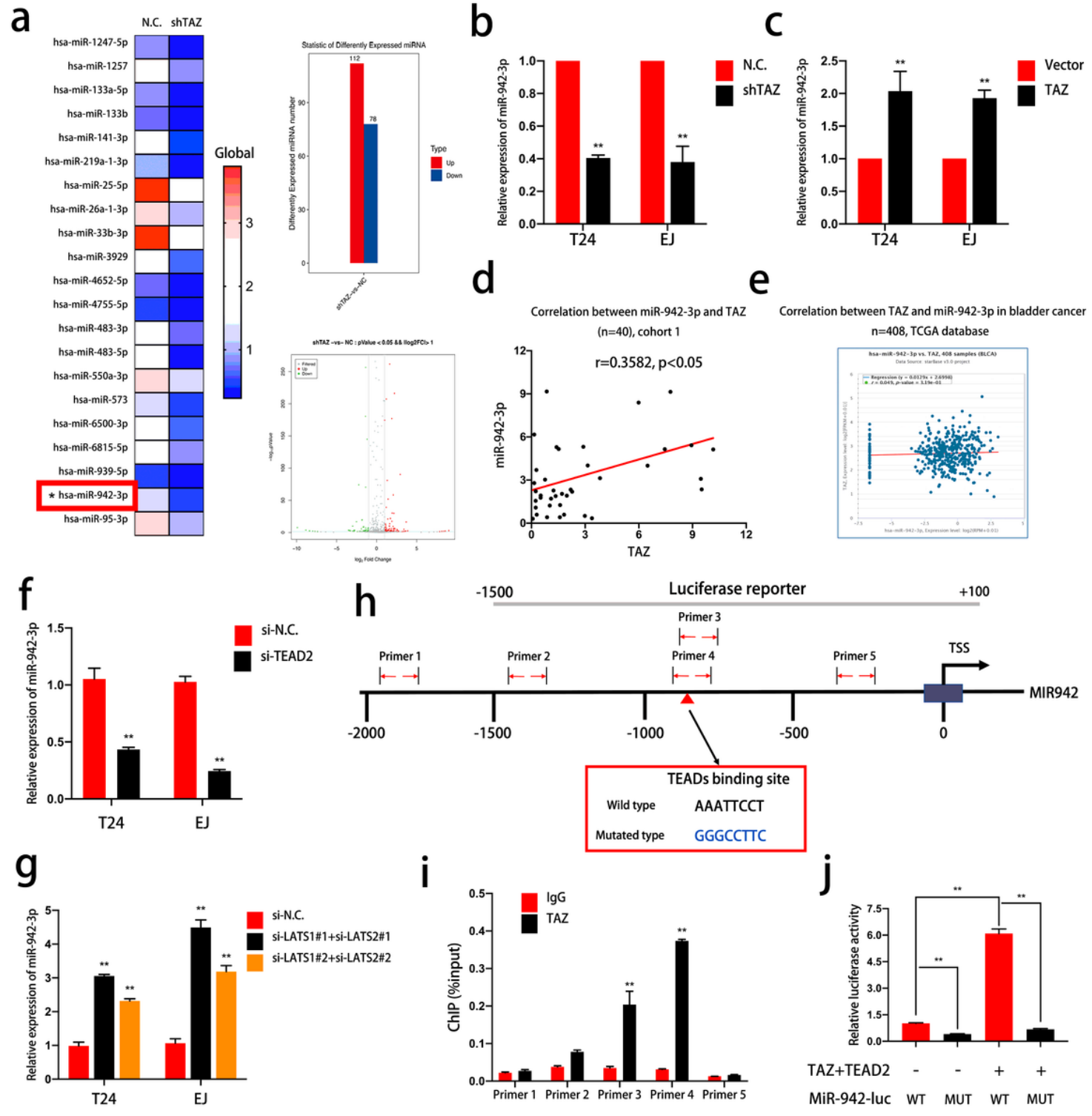

Figure 3

TAZ-TEAD regulates the level of miR-942-3p by binding to its promoter a. TAZ-related miRNAs were identified by RNA sequencing in T24 cells. The heatmap of these miRNAs were generated (N.C. vs shTAZ cells, each sample were mixed with three replicates). b-c qRT-PCR detection of miR-942-3p in TAZ knockdown or overexpressed cells. d-e Correlation between TAZ and miR-942-3p in bladder cancer in cohort 1 and TCGA database. f-g Hippo signaling pathway induces miR-942-3p expression. MiR-942-3p level in LATS1/2-deficient or TEAD2-deficient cells were determined by qRT-PCR. h. Schematic illustration of MIR-942 promoter. Predictive TEADs binding site in the miR-942 promoter (indicated by red arrow). The section of promoter cloned for luciferase reporter assay and primers used for qRT-PCR validation in ChIP assay were indicated. j. Chromatin immunoprecipitation followed by qRT-PCR using specific primers for different regions in miR-942 promoter demonstrated that TAZ could bind to the miR-942 promoter. k. Predicted TEAD binding site was mutated and luciferase reporter assay validated the binding site between TAZ-TEADs and miR-942 promoter. *P < 0.05, **P < 0.01 vs. control group.

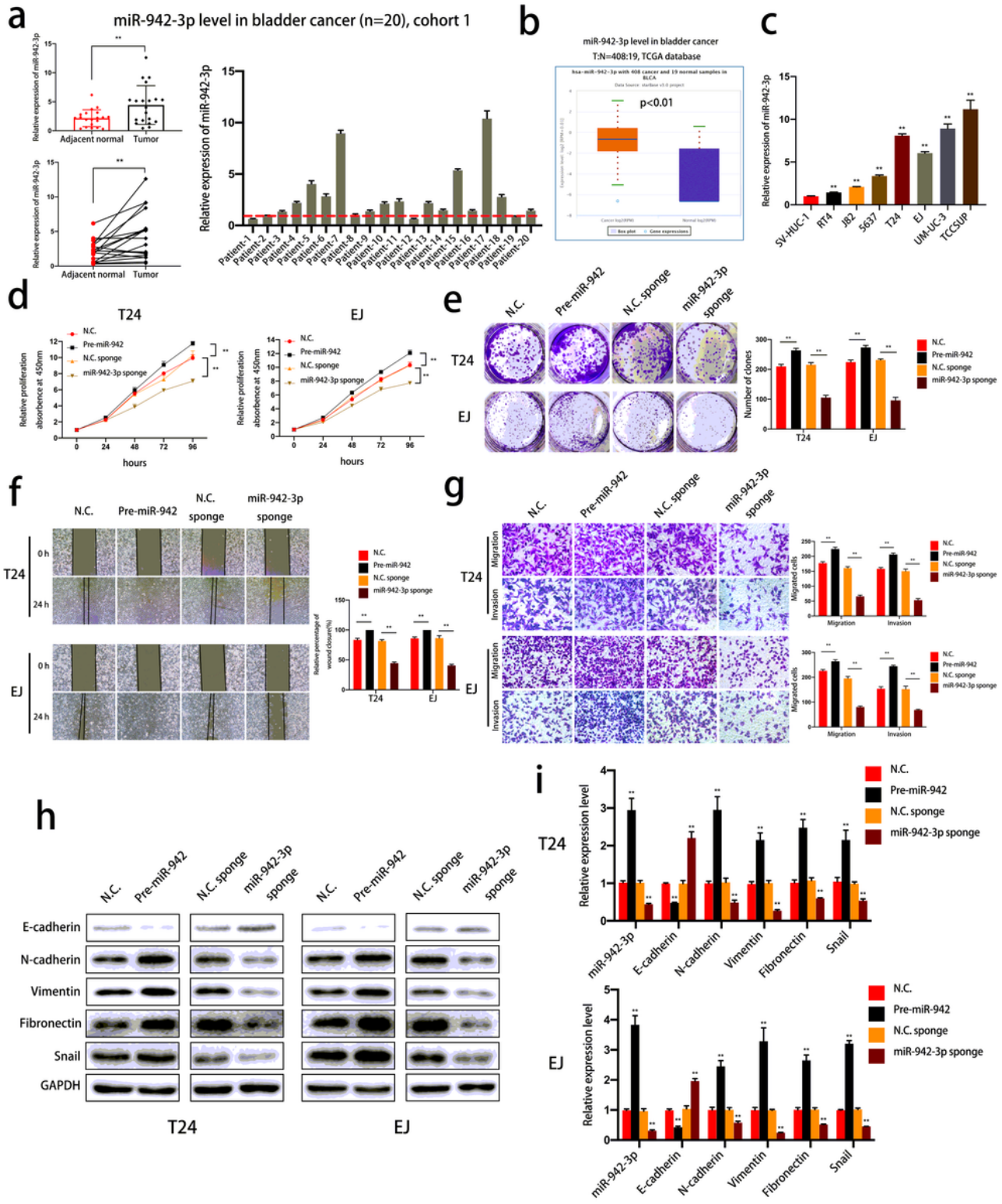

Figure 4

MiR-942-3p is involved in the proliferation, migration, invasion and EMT process of bladder cancer cells a. MiR-433-3p was detected in bladder cancer tissue and adjacent normal tissue (cohort 1, n=20). b. TCGA database indicated the upregulation of miR-942-3p in bladder cancer. c. qRT-PCR was performed to determine miR-942-3p levels in SV-HUC-1 and bladder cancer cell lines. d. Cell viability was measured to evaluate the biological effects of miR-942-3p. e. The effect of miR-942-3p on colony-forming ability was

evaluated by colony formation assay. f. Wound healing assay was performed to evaluate cell migration ability. g. MiR-942-3p influenced the cell migration and invasion ability, as determined by Transwell migration and Matrigel invasion assays. h-i The protein and mRNA expression of EMT markers in T24 and EJ cells transfected with pre-miR-942 or miR-942-3p sponge were detected by western blotting and qRT-PCR, respectively. *P < 0.05, **P < 0.01 vs. control group.

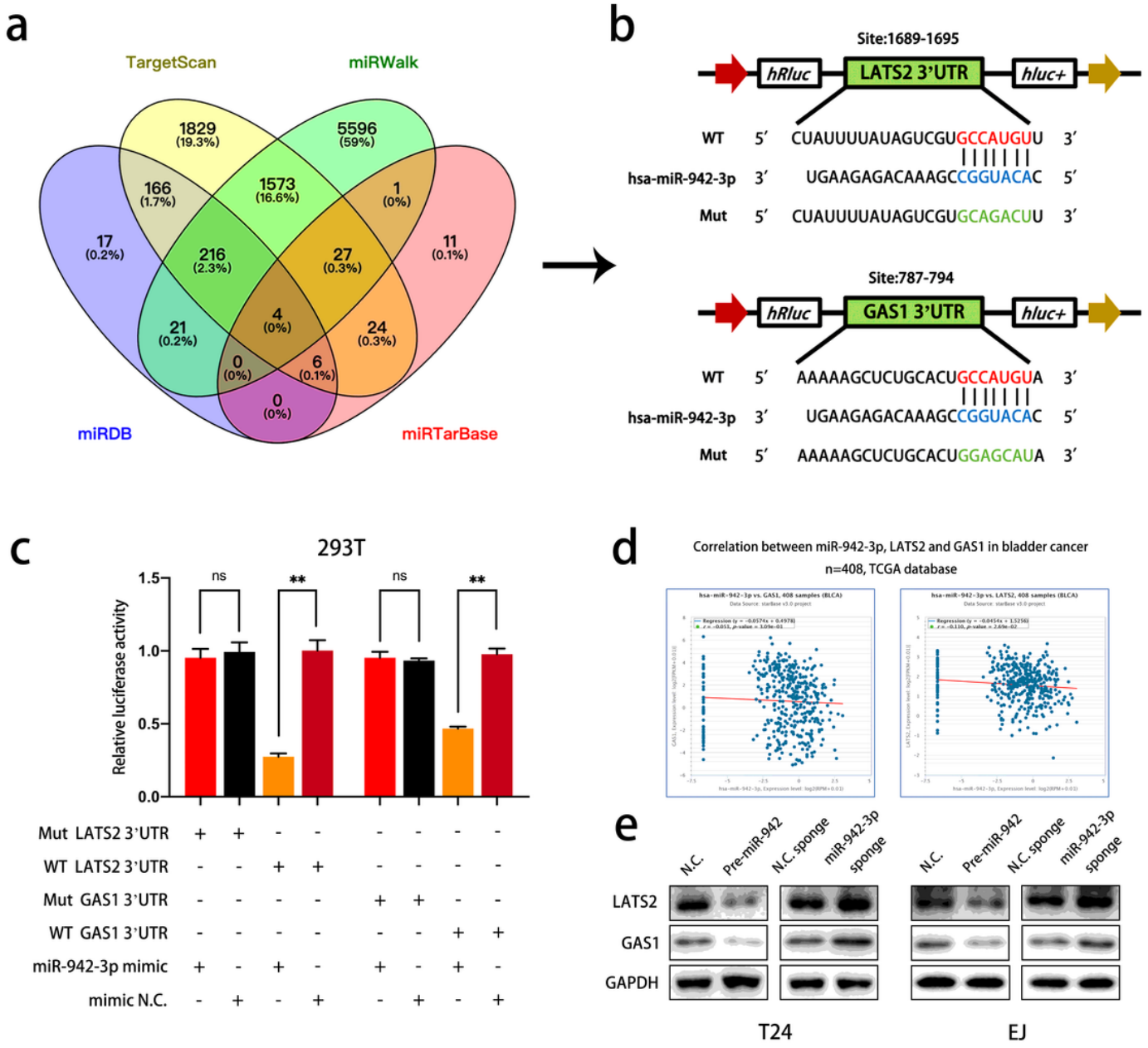

Figure 5

Validation of GAS1 and LATS2 as direct targets of miR-942-3p a. Predicted miR-942–3p target genes by searching the TargetScan, miRDB, miRWalk and miRTarBase databases. b. The potential miR-942-3p binding sites in the 3'-UTR of GAS1 and LATS2 mRNA were showed in the schematic illustration. Lowercase letters indicated the mutated binding sites in the same 3'-UTR. c. Luciferase reporter assay analysis of 293T cells transfected with the indicated plasmids together with miR-942-3p mimics (100

nM). d. TCGA database indicated the negative correlation between miR-942-3p, GAS1 and LATS2. e. MiR-942-3p level was negatively correlated with protein levels of GAS1 and LATS2. *P < 0.05, **P < 0.01 vs. control group.

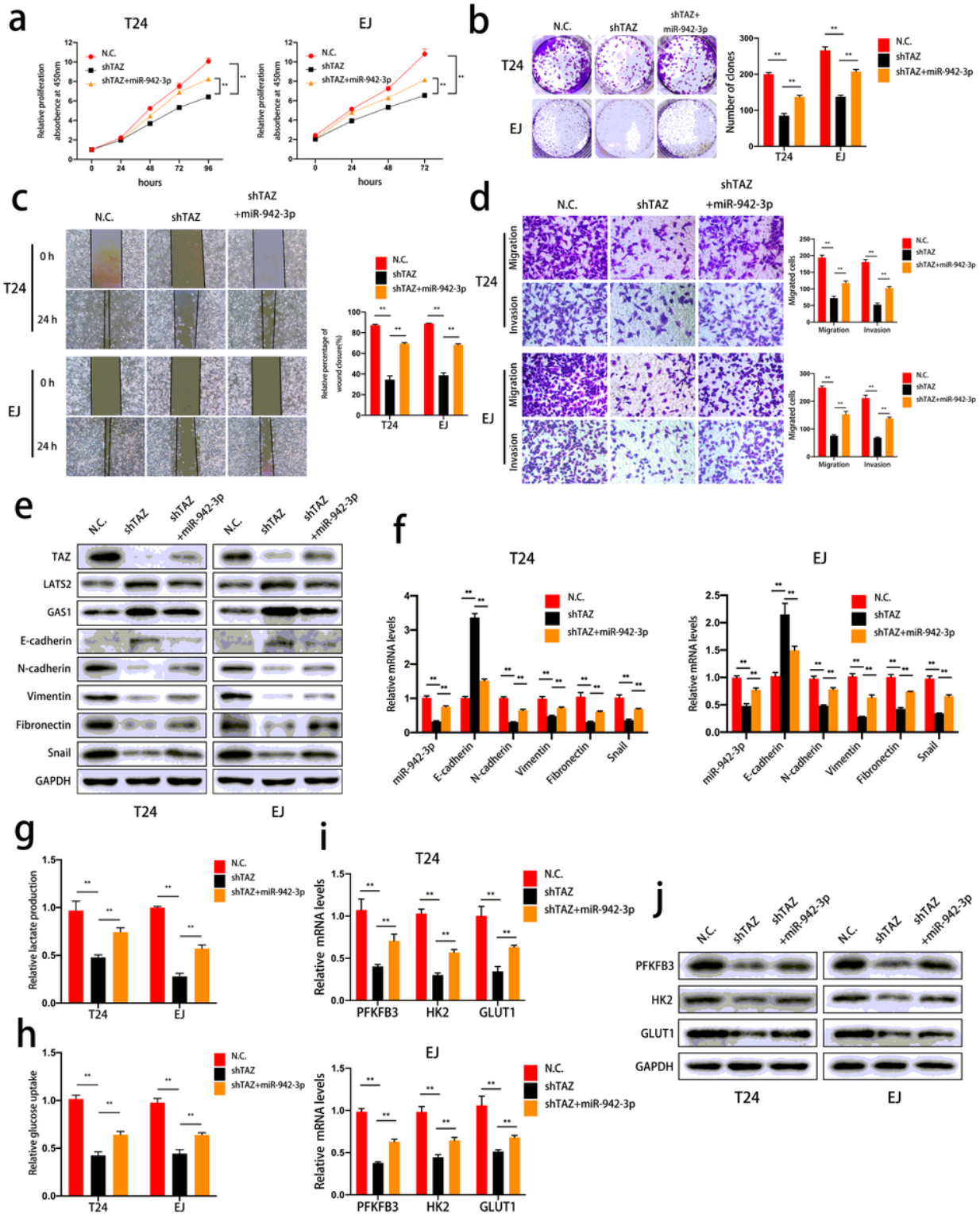

Figure 6

A TAZ/miR-942-3p positive feedback loop modulates the oncogenic effects and glycolysis mediated by TAZ a. Cells were transfected with negative control vector, TAZ shRNA or pre-miR-942. Cell viability was

determined by CCK-8 assay. b. MiR-942-3p promoted the colony formation, as determined by colony formation assay. c. To verify the effects on cell migration, wound healing assay was performed. d. Migration and invasion abilities of bladder cancer cells transfected with different transfectants were evaluated by Transwell migration and invasion assays. e-f The expression levels of TAZ and EMT markers in T24 and EJ cells were evaluated by western blotting and qRT-PCR, respectively. g-h The uptake of glucose and the production of lactate were determined in cells with different condition to evaluate the glycolysis process. i-j The expression levels of glycolysis-related genes (PFKFB3, HK2 and GLUT1) were detected by qRT-PCR and western blotting in TAZ-deficient cells with or without supplement of miR-942-3p. *P < 0.05, **P < 0.01 vs. control group.

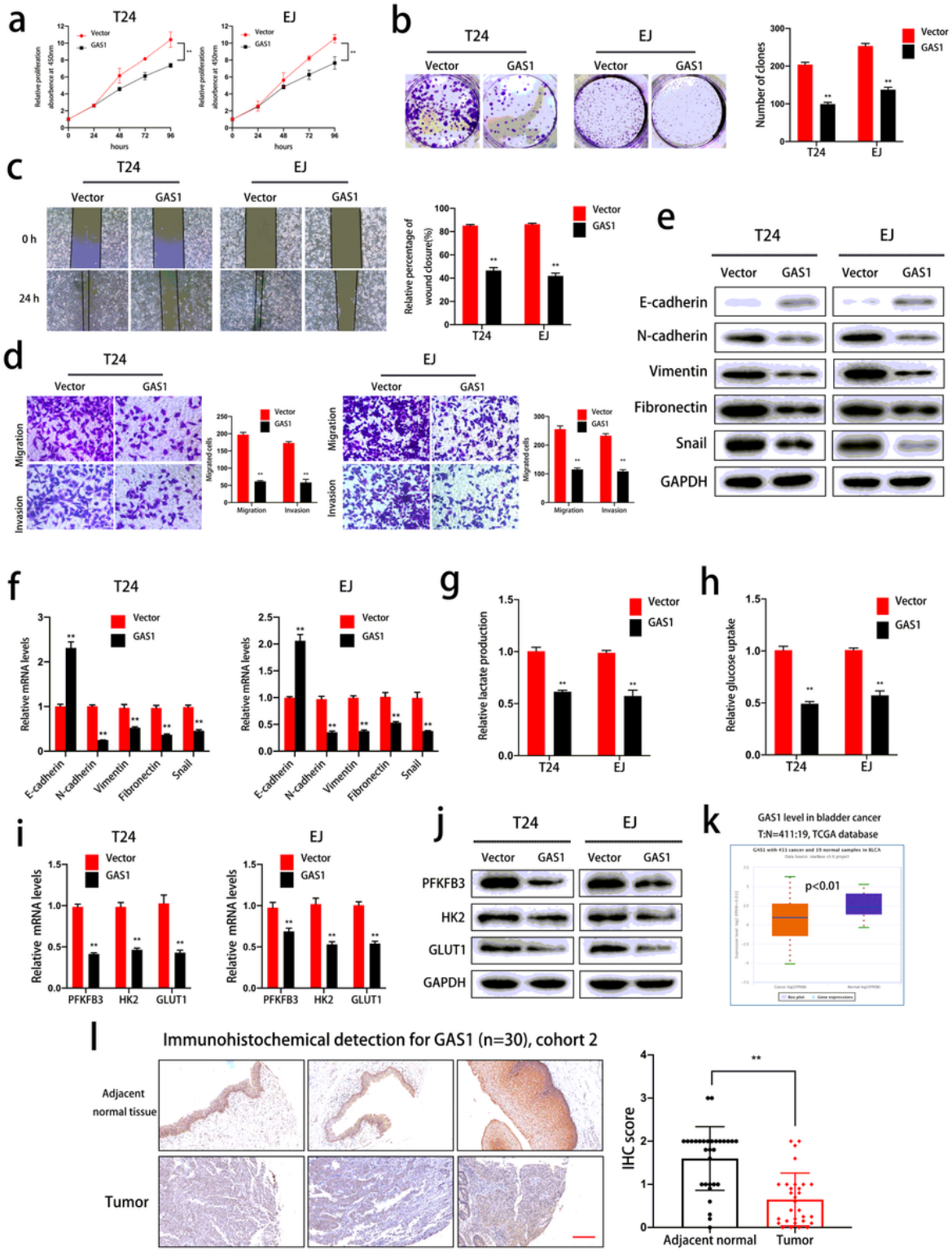

Figure 7

GAS1 overexpression inhibits cell proliferation, migration, invasion, EMT process and glycolysis of bladder cancer cells a. The effect of GAS1 on cell viability was verified by CCK-8 assay. b. Colony formation assay showed that GAS1 impaired the colony forming ability of T24 and EJ cells. c. Wound healing assay indicated the effect of GAS1 overexpression on migration. d. GAS1 overexpression suppressed migration and invasion of T24 and EJ cells, as determined by Transwell migration and

Matrigel invasion assays. e-f Western blot and qRT-PCR analysis showing the expression levels of EMT markers in GAS1 overexpressing bladder cancer cells at protein level and mRNA level. g-h The effects of GAS1 on glycolysis were determined by glucose uptake and lactate production assays. i-j PFKFB3, HK2 and GLUT1 levels were evaluated by western blot and qRT-PCR in GAS1 overexpressing cells. k. TCGA database showed the Lower expression level of GAS1 in bladder cancer tissue compared with normal tissue. l. Immunohistochemical detection of GAS1 in cohort 2 (n=30) further confirmed the dysregulation of GAS1 in bladder cancer. Scale bar: 200 μm. *P < 0.05, **P < 0.01 vs. control group.

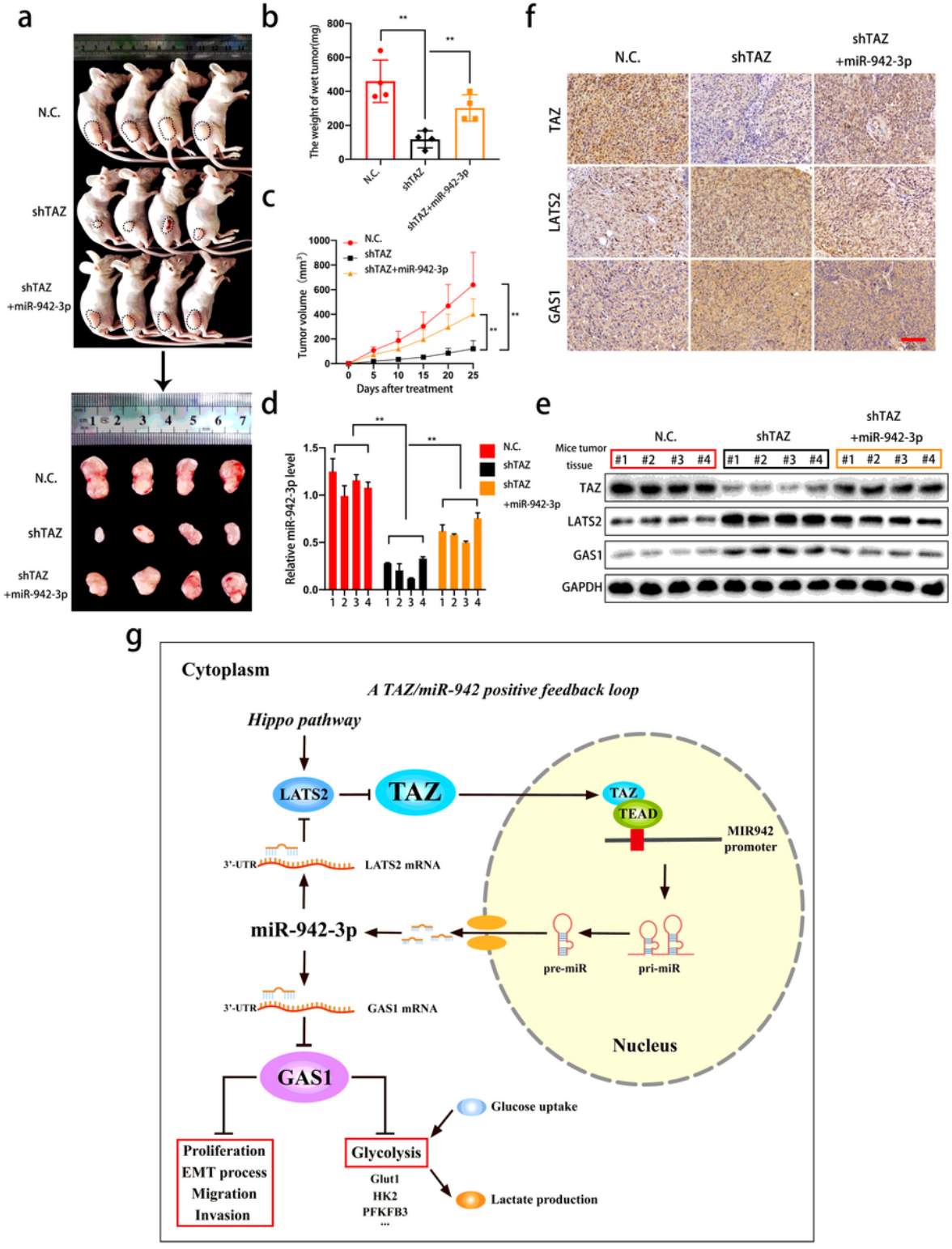

Figure 8

TAZ and miR-942-3p enhance tumor growth of bladder cancer cells in vivo a. An equal number of different T24 cells (negative control, shTAZ or cotransfected with shTAZ and miR-942-3p) were used to establish subcutaneous xenograft tumors. Tumors were harvested and photographed (n=4 each group). b. Tumor weight was determined when the mice were sacrificed. c. Tumor volumes were measured and calculated after the cells were injected into mice. d. MiR-942-3p levels were determined by qRT-PCR in tumors obtained from mice. e. TAZ, LATS2 and GAS1 were detected by western blotting in mice tumor tissues. f. Immunohistochemistry (IHC) detection of TAZ, LATS2 and GAS1 in tumors. Scale bars: 200 μm. g. Schematic diagram illustrating a novel positive feedback loop between TAZ and miR-942-3p that regulates GAS1 expression and modulates biological behaviors, EMT process and glycometabolism in bladder cancer. *P < 0.05, **P < 0.01 vs. control group.

Supplementary Files

This is a list of supplementary files associated with this preprint. Click to download.

- SupplementaryFile1.docx
- SupplementaryFile2.xls